

Out-diffusion of deep donors in nitrogen-doped silicon and the diffusivity of vacancies

V. V. Voronkov and R. Falster

MEMC Electronic Materials, via Nazionale 59, Merano BZ, Italy

(Received 7 February 2012; accepted 30 May 2012; published online 9 July 2012)

A strong resistivity increase in annealed nitrogen-doped silicon samples was reported long ago—but has remained not fully understood. It is now shown that the complicated evolution of the resistivity depth profiles observed can be reproduced by a simple model based on the out-diffusion of some relevant species. Two versions of such an approach were analyzed: (A) out-diffusion of deep donors treated as VN (off-centre substitutional nitrogen), (B) out-diffusion of vacancies (V) and interstitial trimers (N_3) produced by dissociation of VN_3 . Version B, although more complicated, is attractive due to a coincidence of the deduced vacancy diffusivity D_V at 1000 °C with the value extrapolated from low-temperature data by Watkins. © 2012 American Institute of Physics. [<http://dx.doi.org/10.1063/1.4731796>]

I. INTRODUCTION

Nitrogen doping is widely used to control microdefects in Czochralski (CZ) and float-zoned (FZ) crystals and yet the behaviour of nitrogen-related point defects is not quite clear.¹ One puzzling feature is the electrical activity of nitrogen: it is absent in as-grown state but becomes strongly pronounced² after annealing at 900 or 1000 °C. The FZ samples studied in Ref. 2 had, in the as-grown state, a boron-controlled resistivity $\rho_0 = 150 \text{ Ohm cm}$ (corresponding to a hole concentration $p_0 = 8.9 \times 10^{13} \text{ cm}^{-3}$). After annealing, ρ jumped to 20 kOhm cm (a factor of 125) implying that some deep donors were generated in a concentration larger than p_0 resulting in a pinning the Fermi level to a deep donor energy level.

At high temperatures, nitrogen is mostly in the interstitial dimeric (N_2) and monomeric (N_1) states with the minor species N_1 being responsible for nitrogen transport.³ Upon lowering T , monomeric nitrogen is almost completely paired into N_2 . The dimeric state N_2 —observed optically^{2,4}—can be concluded to be electrically inactive. At high T , there is also a substitutional (off-centre) nitrogen species⁵ denoted VN which is a deep centre.⁶ The fraction of this defect at the melting point was estimated⁷ as about 10%. In the samples of Ref. 2, the nitrogen concentration was about $3 \times 10^{15} \text{ cm}^{-3}$ and thus the expected concentration of VN is about $3 \times 10^{14} \text{ cm}^{-3}$ —well above p_0 . Hence, the VN defect is the primary suspect for being the deep donor responsible for the anneal-induced jump in ρ . Apparently, initial VN defects were transformed, during crystal cooling, into some electrically inactive state—most likely by attaching more nitrogen atoms and becoming VN_m species containing m nitrogen atoms. One example of such an inactive defect^{6,8} is VN_2 . It may be expected that other even-sized species VN_4 , VN_6 , etc., are also electrically inactive since they are combined of electrically inactive defects VN_2 and N_2 .

During subsequent annealing, the grown-in VN_m species (of even m) are expected to convert back into the high-temperature dominant form VN—deep donors. So far so

good. However, this concept is very hard to reconcile⁹ with the observed evolution of the resistivity depth profile $\rho(z)$ (which was monitored² by spreading resistance profiling (SRP)). The measured profiles after 1000 °C annealing are shown in Fig. 1 by circles. There is a donor-depleted region close to the sample surface—narrow after 1 min but much wider after 4 min. After 8 min, the donors disappear completely (the resistivity ρ returns to its initial value ρ_0). To account for these profiles, an extremely complicated model has been developed.⁹ In it, in the first place, it should be assumed that the grown-in inactive VN_m species are transformed not directly to the stable form VN but rather to a metastable forms like VN_3 . The VN_3 donors are annihilated by in-diffusing self-interstitials (I) by $I + VN_3$ reaction. This produces mobile interstitial trimers N_3 which then out-diffuse and precipitate at the surface—resulting in the emission of I by the nitride precipitates. Each of the two mobile species, I and N_3 , is thus created by the other one. An obtained fit was satisfactory but involved a very large number of fitting parameters.

In the present study, a much simpler model of the deep donor loss—entirely based on out-diffusion process—was tried. Before specifying the details, the simulated profiles are shown in Fig. 1 by solid curves, to make it clear that the computed profiles inevitably show a smooth variation in $\rho(z)$ through the whole depth. This is in contrast to the reported plateau in the central sample portion which had a fixed value $\rho_{\text{max}} = 20 \text{ kOhm cm}$ (found also after 900 °C anneal). This persistent plateau was actually the main difficulty that necessitated the complicated model of self-interstitial in-diffusion⁹ in order to annihilate the donors only up to some limited depth. This difficulty is however removed if ρ_{max} is not the true resistivity but rather simply the upper limit of the SRP instrument used in Ref. 2. In this case, only the profile parts with $\rho(z) < \rho_{\text{max}}$ are meaningful, and only these parts are to be fitted—as was done in Fig. 1. The fit is better than that achieved before.⁹

Two qualitatively different models of the out-diffusion process were tried as outlined below.

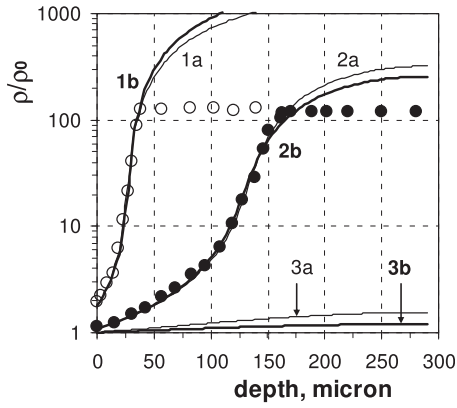


FIG. 1. Resistivity depth profiles² measured in nitrogen-doped FZ samples annealed at 1000 °C for 1 and 4 min (open and closed circles). The solid curves numbered 1 to 3 are computed for 1, 4, and 8 min anneal, respectively, within two different out-diffusion models (thin curves 1a to 3a are for model A, and the thick curves 1b to 3b—for model B).

II. MODEL A: OUT-DIFFUSION LOSS OF VN

In this version of an out-diffusion concept, the grown-in neutral species (VN_m) are instantaneously converted—at 1000 °C—back into the original state VN. At the start of anneal, these donors have a uniform concentration N_0 expected to be $\approx 3 \times 10^{14} \text{ cm}^{-3}$.

The loss of VN may then proceed through dissociation into $V + N_1$, with subsequent out-diffusion of vacancies. This process is a trap-limited vacancy out-diffusion, with N_1 atoms as traps of a concentration maintained by the major interstitial species N_2 through a fast dissociation/pairing reaction $N_2 \leftrightarrow 2 N_1$. The concentration of N_2/N_1 is strongly reduced (by the out-diffusion of N_1) within a narrow near-surface region of about 20 μm after an anneal of several minutes.¹⁰ Accordingly, [VN] would be also reduced in this narrow region in comparison to a deeper part where N_2 is not yet lost. The resistivity profile however shows no such a peculiarity: it decreases steadily towards the surface “not noticing” a narrow near-surface nitrogen-depleted region (Fig. 1).

Therefore, the VN loss cannot be attributed to trap-limited vacancy out-diffusion. This conclusion is consistent with a negligible rate of the dissociation reaction $VN \rightarrow V + N_1$ inferred from the nitrogen effect on the grown-in microdefects.¹

The remaining loss mechanism of VN is then out-diffusion of VN themselves. There is an analogous species VO (substitutional off-centre oxygen) that is mobile as evidenced by its reaction with oxygen to produce VO₂ at relatively low T —when oxygen itself is practically immobile.¹¹ The deduced diffusivity of VO, when extrapolated to 1000 °C, equals $\approx 2.5 \times 10^{-8} \text{ cm}^2/\text{s}$. The diffusivity of VN deduced below, $2 \times 10^{-6} \text{ cm}^2/\text{s}$, is not dramatically higher. Hence an assumption of a mobile VN species does not seem to be unrealistic.

The donor depth profile $N(z, t)$ then evolves by simple diffusion equation, with a diffusivity D . The computed donor concentration should be converted into the measured quantity, the resistivity ρ , which is inversely proportional to the hole concentration p —since the hole mobility, for lightly doped p-Si, has a fixed value. Hence $\rho/\rho_0 = p_0/p$. The hole

concentration p is expressed through p_0 and N by the neutrality equation

$$p + N^+ = p_0. \quad (1)$$

The concentration of charged donors N^+ is controlled by the Fermi level position with respect to the donor level E or equivalently¹² by the equation

$$N^+ = Np/(p + p_d), \quad (2)$$

where p_d is the characteristic hole concentration for the Fermi level coincident with the energy level E (referenced from the top of the valence band)

$$p_d = g N_v \exp(-E/kT). \quad (3)$$

Here N_v is the state density in the valence band (at T_{room}) and g is the degeneracy factor, on the order of 1. The parameter deduced by fitting is p_d . The energy level E can then be estimated by Eq. (3).

The near-surface resistivity is somewhat larger than the as-grown value (Fig. 1) which can be attributed to a time-dependent boundary condition. For the sake of simplicity, an exponential decay in the boundary donor concentration $N_s(t)$ is assumed

$$N_s(t) = N_{s0} \exp(-t/\tau). \quad (4)$$

By the two values of the near-surface resistivity (after 1 and 4 min in Fig. 1), the parameters in Eq. (1) are: $\tau = 1.7 \text{ min}$, $N_{s0} = 7 \times 10^{13} \text{ cm}^{-3}$.

The computed profiles of Fig. 1 (thin curves 1a to 3a) are obtained with the following best-fit parameters: $N_0 = 4 \times 10^{14} \text{ cm}^{-3}$ (quite close to the expected value), $D = 2.1 \times 10^{-6} \text{ cm}^2/\text{s}$ and $p_d = 1.7 \times 10^{11} \text{ cm}^{-3}$ (which corresponds to the donor level at $\approx E_v + 0.45 \text{ eV}$). It is also informative to show the depth profiles of VN donors (Fig. 2). The apparent depth of the donor-depleted region is defined by intersection of $N(z, t)$ with horizontal (dashed) line showing the value of p_0 . Due to a relatively high D , the VN concentration is reduced through the whole wafer depth already

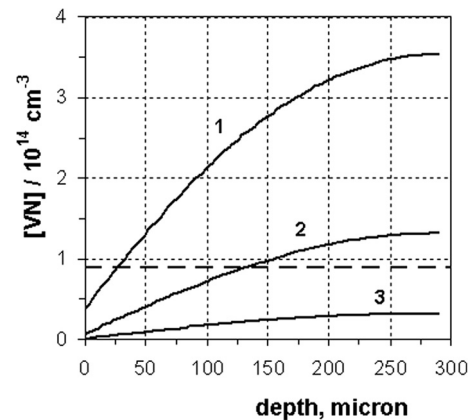


FIG. 2. Computed depth profiles of deep donors VN (model A). The curves 1, 2, and 3 correspond to annealing at 1000 °C for 1, 4, and 8 min, respectively.

after 4 min. This accounts for a propagation of the depleted region at a far faster velocity than that by a normal diffusion law $t^{1/2}$. After 8 min (the curve 3 in Fig. 2), the donor concentration is reduced severely, and the corresponding resistivity (curve 3a in Fig. 1) becomes close to the initial value ρ_0 . Yet ρ/ρ_0 is still somewhat larger than 1, in a slight discrepancy with the experiment² that shows complete coincidence of ρ with ρ_0 after 8 min anneal at 1000 °C.

III. MODEL B: DISSOCIATION LOSS OF VN_3

The model described above is attractive because of its simplicity but nonetheless leaves an uneasy feeling ascribing a high diffusivity to the off-centre substitutional nitrogen VN. An alternative model can be based on the peculiar shape of nitrogen out-diffusion profile:¹³ apart from the major slow-diffusing N_2/N_1 component, there is also a fast-diffusing component. The latter was attributed to a fast out-diffusion of nitrogen trimers N_3 that exist independent of the major N_2/N_1 component and originate from the annihilation reaction of VN_3 defects with in-diffusing self-interstitials. Now, within the out-diffusion concept, the trimers N_3 are supposed to be produced by the dissociation reaction $\text{VN}_3 \rightarrow \text{V} + \text{N}_3$. This leads to an appreciable vacancy supersaturation. The self-interstitial concentration is accordingly under-saturated—which makes a self-interstitial contribution into defect transport inessential. The source defects for the trimers, VN_3 , originate from the grown-in VN_m neutral species which means that these species, upon heating, do not return to the stable high-temperature form VN but rather transform into metastable species VN_3 .

The first question is: which of the three species involved (VN_3 , V, and N_3) is the deep donor responsible for a resistivity jump?

The vacancy is either neutral or negative¹⁴ in p-Si at T_{room} . During a post-anneal quench, V can be trapped by N_2 (the major defect in nitrogen-doped FZ samples). The stable VN_2 complex is electrically inactive^{6,8} but there could be a metastable configuration VN_2^* produced during a quench. Yet it is highly unlikely that this hypothetical defect—combined of a neutral N_2 and a neutral (or negative) V—is a donor.

The next tentative identification of the deep donors is with VN_3 . This however does not allow a quantitative fitting of the resistivity profiles. The VN_3 concentration, in equilibrium with V and N_3 , is specified by a mass-action law

$$[\text{V}][\text{N}_3]/[\text{VN}_3] = K_3, \quad (5)$$

where K_3 is the equilibrium dissociation constant. Both [V] and $[\text{N}_3]$ decrease towards the sample surface linearly, due to out-diffusion. Thus, $[\text{VN}_3]$ decreases by a parabolic law—inconsistent with the quasi-linear near-surface portions of the resistivity profiles in Fig. 1.

Therefore, the only suitable identification of the deep donors is N_3 . The VN_3 species are also treated as donors but of an energy level essentially below that of N_3 and thus having only a slight impact on ρ . The out-diffusion process is now described by 3 parameters: two diffusivities (D_V of V

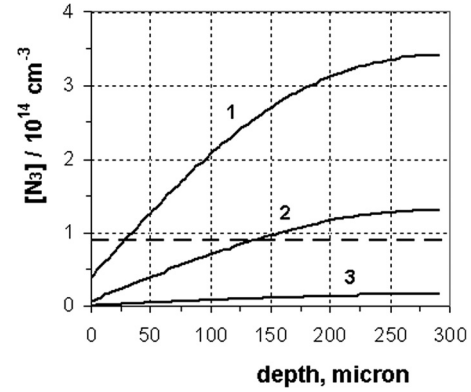


FIG. 3. Computed depth profiles of deep donors N_3 (model B) for annealing at 1000 °C. The curves 1, 2, and 3 correspond to the anneals of 1, 4, and 8 min, respectively.

and D_3 of N_3) and the dissociation constant K_3 . The computed profiles are very sensitive to all the three parameters, and therefore all of them were unambiguously deduced by the fitting of the measured curves in Fig. 1: $D_V = 2.3 \times 10^{-5} \text{ cm}^2/\text{s}$, $D_3 = 3.2 \times 10^{-6} \text{ cm}^2/\text{s}$, $K_3 = 10^{14} \text{ cm}^{-3}$. Remarkably, the deduced value of D_V is very close to the value of $2 \times 10^{-5} \text{ cm}^2/\text{s}$ extrapolated to 1000 °C from low-temperature radiation data.¹⁵ The best-fit value of the concentration p_d for the deep donor N_3 is about $1.3 \times 10^{11} \text{ cm}^{-3}$ (corresponding to the donor level at $\approx E_V + 0.46 \text{ eV}$).

The best-fit resistivity profiles at 1000 °C for 1 and 4 min (the thick curves 1b and 2b in Fig. 1) are practically indistinguishable from those obtained within the previous model for the meaningful curve portions, $\rho < \rho_{\text{max}}$. However, after 8 min, the resistivity (curve 3b in Fig. 1) is somewhat lower and more consistent with the experimental results² that give a value of unity for ρ/ρ_0 after 8 min. The computed depth profiles of N_3 are shown in Fig. 3. Initially the VN_3 , V, and N_3 species are present in a proportion 0.65:0.35:0.35. The initial amount of N_3 is essentially smaller than N_0 and yet higher than p_0 and thus enough to pin the Fermi level at the deep level of N_3 . Upon annealing, the $[\text{V}]/[\text{N}_3]$ ratio decreases due to a higher diffusivity of V. Accordingly, the ratio of the two donors, $[\text{VN}_3]/[\text{N}_3]$ —specified by Eq. (5)—is reduced; it becomes < 1 already after 1 min, and $\ll 1$ after 4 min. A contribution of VN_3 into the resistivity is insignificant even at the shortest time of 1 min. For this reason, the value of p_d for VN_3 can be estimated only roughly: it is on the order of 10^{15} cm^{-3} . The corresponding level is at $E_V + 0.23 \text{ eV}$.

IV. GENERATION AND LOSS OF DEEP DONORS AT 900 °C

The reported resistivity depth profiles induced by annealing at 900 °C are much more complicated (Fig. 4). Clearly, transformation of grown-in VN_m species into VN (for model A) or into VN_3 (for model B) is no longer instantaneous but takes several minutes. Only after 8 min anneal, the resistivity reaches a high value, the same as that produced immediately at 1000 °C. To account for the profiles, it is necessary to assume that some intermediate donor species—different from those discussed above—are produced

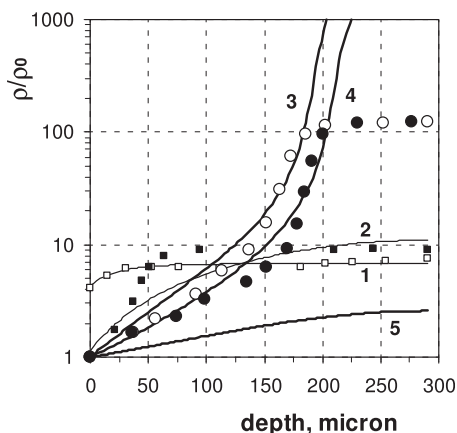


FIG. 4. Resistivity depth profiles² produced by annealing at 900°C for 1 min (open squares), 4 min (filled squares), 8 min (open circles), and 16 min (filled circles). The solid curves 1 to 5 (for annealing time of 1, 4, 8, 16, and 32 min, respectively) are computed within a modified version of model B that includes transient formation of donor species that later transform into VN_3 .

within this transient time. It means that additional—and highly speculative—assumptions on the kinetics of VN_m conversion have to be made to describe the profiles. An example, for the model B, is shown by the solid curves in Fig. 4; the fit quality is not yet quite satisfactory for the shorter times of 1 and 4 min. For this reason, the model parameters deduced by the fitting procedure are not as reliable as for 1000°C case, and they will not be discussed in detail. It is only worth noting that the profiles for 8 and 16 min, can be qualitatively explained by the model B as follows. The dissociation constant K_3 at 900°C is essentially smaller than at 1000°C, and hence the concentration of deep donors N_3 is initially low—less than p_0 —and insufficient to induce a strong rise in ρ . Only later, due to a reduction in $[\text{V}]$ by a fast vacancy out-diffusion does the fraction of N_3 increase—by Eq. (5)—becoming sufficient for a resistivity jump as was observed after 8 and 16 min. In the interval between 8 and 16 min, a loss of $[\text{VN}_3]$ is accompanied by an increase in the $[\text{N}_3]/[\text{VN}_3]$ ratio, and the concentration $[\text{N}_3]$ of the major deep donors is not changed much, which accounts for almost identical resistivity profiles after 8 and 16 min. Only for longer anneals, the model predicts an essential reduction in $[\text{N}_3]$ and hence in the resistivity (Fig. 4, curve 5). The vacancy diffusivity required to reproduce the profiles at 900°C is about $3.8 \times 10^{-6} \text{ cm}^2/\text{s}$ —remarkably smaller than the extrapolated value of Watkins. This may be attributed to vacancy trapping by the major nitrogen species N_2 —well pronounced at lower T . The deduced vacancy diffusivity is then an effective value equal to the true diffusivity multi-

plied by a fraction of free mobile vacancies in the $\text{V} + \text{VN}_2$ community. Roughly, this fraction is estimated as 0.3 at 900°C.

V. SUMMARY

The reported resistivity profiles in annealed nitrogen-doped samples² include a plateau of a high resistivity, ρ_{max} . Such a shape is very hard to reproduce by simulations. However, once ρ_{max} is treated as an instrumental limit rather than the true resistivity, the genuine parts of the profiles (with $\rho < \rho_{\text{max}}$) are successfully fitted by a simple model based on an out-diffusion process. Two versions of this process were considered:

- The deep donors are VN (substitutional off-centre nitrogen), and they are mobile. There is a known example of an analogous species—substitutional off-centre oxygen, VO—that is mobile too, although its diffusivity is lower by two orders of magnitude (in the same temperature range).
- The species produced by annealing are VN_3 rather than VN and they are lost through dissociation into two mobile species: vacancies V and interstitial nitrogen trimers N_3 . The deep donors are identified as N_3 .

The version A is attractive by its simplicity while B is by virtue of a remarkable coincidence of the deduced vacancy diffusivity with the Watkins value¹⁵ extrapolated from cryogenic temperatures. A marginal advantage of the model B is that it predicts a stronger loss of donors after 8 min anneal at 1000°C.

An apparent next step is to use the out-diffusion models to simulate quantitatively the available nitrogen out-diffusion profiles.

¹V. V. Voronkov and R. Falster, *Solid State Phenom.* **131–133**, 219 (2008).

²T. Abe, H. Harada, N. Ozawa, and K. Adomi, *Mater. Sci. Res. Symp. Proc.* **59**, 537 (1986).

³V. V. Voronkov and R. Falster, *Solid State Phenom.* **95–96**, 83 (2004).

⁴H. J. Stein, *Mater. Sci. Res. Symp. Proc.* **59**, 523 (1986).

⁵K. L. Brower, *Phys. Rev. B* **28**, 6040 (1982).

⁶J. P. Goss, J. Hahn, R. Jones, P. R. Briddon, and S. Oberg, *Phys. Rev. B* **67**, 045206 (2003).

⁷V. V. Voronkov and R. Falster, *J. Cryst. Growth* **273**, 412 (2005).

⁸H. Sawada and K. Kawakami, *Phys. Rev. B* **62**, 1851 (2000).

⁹V. V. Voronkov and R. Falster, *Thin Solid Films* **518**, 2346 (2010).

¹⁰T. Itoh and T. Abe, *Appl. Phys. Lett.* **53**, 39 (1988).

¹¹B. G. Swensson and J. L. Lindstrom, *Phys. Rev. B* **34**, 8709 (1986).

¹²J. S. Blackmore, *Semiconductor Statistics* (Pergamon, NY, 1962).

¹³V. V. Voronkov and R. Falster, *ECS Trans.* **3**, 113 (2006).

¹⁴G. D. Watkins, *ECS Proc.* **99–1**, 38 (1999).

¹⁵G. D. Watkins, *J. Appl. Phys.* **103**, 106106 (2008).